Heating and cooling processes via phaseonium-driven dynamics of cascade systems

Federico Amato,[1, *] Claudio Pellitteri,[2] G. Massimo Palma,[2, 3] Salvatore Lorenzo,[2] and Rosario Lo Franco[1]

[1]*Dipartimento di Ingegneria, Università degli Studi di Palermo,*
Viale delle Scienze, 90128 Palermo, Italy
[2]*Dipartimento di Fisica e Chimica - Emilio Segrè, Università degli Studi di Palermo,*
via Archirafi 36, I-90123 Palermo, Italy
[3]*NEST, Istituto Nanoscienze-CNR, Piazza S. Silvestro 12, 56127 Pisa, Italy*
(Dated: December 8, 2023)

The search for strategies to harness the temperature of quantum systems is one of the main goals in quantum thermodynamics. Here we study the dynamics of a system made of a pair of quantum harmonic oscillators, represented by single-mode cavity fields, interacting with a thermally excited beam of phaseonium atoms, which act as ancillas. The two cavities are arranged in a cascade configuration, so that the second cavity interacts with phaseonium atoms only after their interaction with the first one. We provide exact closed dynamics of the first cavity for arbitrarily long interaction times. We highlight the role played by the characteristic coherence phase of phaseonium atoms in determining the steady states of the cavity fields as well as that of the ancillas. Also, we show how the second cavity follows a non-Markovian evolution due to interactions with the "used" ancillary atoms, that enables information exchange with the first cavity. Adjusting the parameters of the phaseonium atoms, we can determine the final stable temperature reached by the cavities. In this way, the cavities can be heated up as well as cooled down. These results provide useful insights towards the use of different types of ancillas for thermodynamic cycles in cavity QED scenarios.

I. INTRODUCTION

Since the introduction of the *phaseonium* by Scully in [1], this new "state of matter" gave birth to interesting applications, from the early adoptions as a mean for lasing without inversion, refractive index enhancement and correlated spontaneous emission lasers [2], to its later use in a single-heat-bath quantum Carnot engine [3]. Its optical properties were reviewed and developed later on [4, 5], while applications have been proposed for its optomechanic properties [6] and for its role as quantum fuel [7]. Phaseonium is a three-level lambda system with two almost-degenerate ground states in a coherent superposition. As simple as it is, the characteristic quantum property of coherence often leads to unexpected and interesting consequences, giving the phaseonium its appeal.

Here, we study the phaseonium as thermal bath coupled to a multipartite system, within the framework of collision models (CMs) [8, 9]. As a paradigmatic continuous-variable (CV) system, we consider the one composed of two harmonic oscillators, which are physically represented by two single-mode cavities. We follow phaseonium atoms as they interact with the two subsystems (cavities) one after another, in what is called *cascade* configuration [10–16]. We give the exact time evolution of the system and see how the atoms of the bath mediate a one-way information flow between the subsystems. Consequently, while we can trace out the reduced dynamics of the first cavity alone, as it does not "see" the second one, the last cavity follows a non-Markovian reduced dynamics. Although collision models usually end up taking the continuous-time limit of the model, we leave on purpose the description of the dynamics to be *discrete*.

The interaction time between phaseonium and system at discrete time-steps plays the role of a control parameter for the overall dynamics, and the effects of gauging it are thus investigated. Accounting for this, we follow the arguments of Ref. [17] to provide the finite-time quantum map for the system without approximations. As a result, the two cavities reach a thermal state at the same temperature. We point out that this thermalization process, described by a finite difference master equation, is controlled by the coherence phase of the phaseonium bath atoms.

The paper is structured as follows. In Section II we present a brief review of the theoretical framework of CMs to tackle open quantum systems' dynamics. In Section III we describe an optical cavity and the phaseonium atoms with their operators and free-evolution Hamiltonians, as well as their interaction, which constitute the foundation of this work. In Section IV, we carve out from the cavity-phaseonium interaction the Kraus operators that form the dynamical map for the cavity evolution, giving the stationary conditions and the expressions for long-time stationary states for both cavity and ancillas. In Section V we describe the cascade system and its dynamical map with appropriate Kraus operators. A detailed graphical analysis of the thermalization process of the cavities is given in Section VI, by following the evolution of their temperatures at each collision step. As a remarkable application, we highlight that the system can be heated up or cooled down to a stable chosen temperature, setting suitable parameters of the incoming phaseonium atoms. To assess the robustness of this process, we also take into account the effects due to stochastic noise in the interaction time or in the coherence phase. Finally, in Section VII we discuss the results in a broader context, from both experimental and theoretical prospects.

II. QUANTUM COLLISION MODELS

In this section, we briefly recall the collision model approach [8] to open quantum systems' dynamics [18]. Gen-
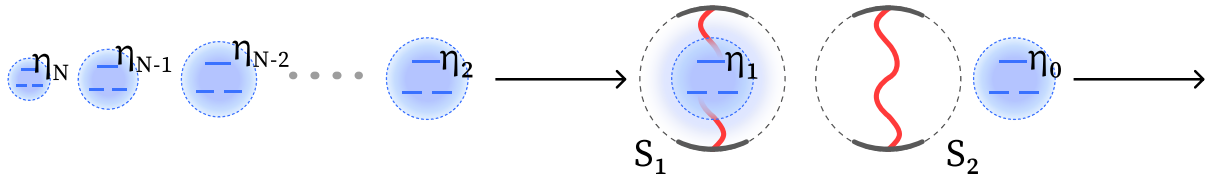
FIG. 1. Standard collision model for a phaseonium bath interacting with a multipartite system. The system of interest is a cascade of two single-mode cavity fields S_1, S_2, which is described by a density operator ρ. The environment is made up of N three-level atoms in lambda configuration, called phaseonium atoms, all prepared equally. These atoms play the role of ancillas and are described by a density operator η_k ($k = 0, \ldots, N$). Ancillas travel at speed v and enter the cavities at a rate r. They interact with each cavity field for a time Δt. The speed and rate of phaseonium atoms is selected such that there is at most one ancilla in each cavity at a time.

erally speaking, the dynamics of a quantum system S is said *open* when the system is coupled to a bath B whose time evolution cannot be investigated or is inaccessible. In the simplest collision model, the bath B is taken as a large discrete collection of elementary systems—called *ancillas*—that interact *one at a time* with the system, where each of these *collisions* is described by unitary two-body interactions. Such a collision model decomposes the complex system-bath dynamics into simple contributions. An intuitive implementation of collision models is, for example, the *micromaser* [19, 20].

The initial joint state of the bath B, made up of identical ancillas η_k ($k = 1, 2, \ldots, N$), and the system S is assumed to be a product state $\chi_0 = \rho_0 \otimes \eta_1 \otimes \eta_2 \otimes \ldots \otimes \eta_N$. One by one, ancillas collide with the system for a short time Δt at discrete time steps labelled by the same k as that of the colliding ancilla. The dynamics is thus discrete. Let us denote with $\hat{H}_S$ and $\hat{H}_\eta$ the free Hamiltonians of S and the k-th ancilla η_k, respectively, which define the total Hamiltonian $\hat{H}_0 = \hat{H}_S + \hat{H}_\eta$. Indicating the system-ancilla interaction with $\hat{V}_k$, the dynamics of each k-th collision is ruled by the unitary evolution operator

$$\hat{U}_k = e^{-i\Delta t(\hat{H}_S + \hat{H}_\eta + \hat{V}_k)} . \tag{1}$$

Three assumptions are now required to ensure a Markovian behaviour of the model (i.e., governed by a master equation in Lindblad form):

- ancillas do not interact with each other;

- ancillas are initially uncorrelated;

- each ancilla collides with S only once.

At each step, the whole state evolves according to $\chi_k = \hat{U}_k \chi_{k-1} \hat{U}_k^\dagger$, starting from $\chi_1 = \hat{U}_1 \chi_0 \hat{U}_1^\dagger$. The corresponding state of the system at each step, ρ_k, is obtained tracing out the ancillas' degrees of freedom. Using the partial trace Tr_j over the degrees of freedom of the j-th ancilla, one finds, recursively,

$$\rho_k = \text{Tr}_\mathcal{B}\{\chi_k\} = \text{Tr}_k\{\hat{U}_k \cdots \text{Tr}_1\{\hat{U}_1 \rho_0 \otimes \eta_1 \hat{U}_1^\dagger\} \cdots \otimes \eta_k \hat{U}_k^\dagger\}.$$

This suggests defining the quantum *collision map* $\mathcal{E}$ as

$$\rho_k = \mathcal{E}[\rho_{k-1}] = \text{Tr}_k\{\hat{U}_k(\rho_{k-1} \otimes \eta_k)\hat{U}_k^\dagger\}, \tag{2}$$

which shows that the state of S at step n only depends on that at the previous step $n - 1$: the dynamics has *no memory* of

its past history, as is expected for Markovian dynamics (see, for instance, Ref. [21], for a review on Markovian and non-Markovian processes with memory effects).

The steady state ρ^* of the system is obtained by the *fixed point* of the dynamical map, that is the state such that $\mathcal{E}[\rho^*] = \rho^*$. If the fixed point is unique, the collision map is *ergodic*. Moreover, if any initial state ρ_0 eventually tends to the same steady state ρ^*, the map is said to be *mixing* [22–24].

III. SYSTEM AND PHASEONIUM BATH

We begin our discussion introducing the main actors: the open system we want to look at and the environment in which it is positioned. Figure 1 depicts the model of interest for a cascade two-cavity system interacting with a beam of phaseonium atoms, which will be analysed in Sec. V.

Here, we start considering a single-mode optical cavity as system S. The cavity behaves like a single-mode harmonic oscillator whose Hamiltonian is [18]

$$\hat{H}_S = \hbar\omega_c\left(\hat{a}^\dagger\hat{a} + \frac{1}{2}\right) , \tag{3}$$

where $\hat{a}^\dagger$ and $\hat{a}$ are, respectively, the creation and annihilation operators stemming from the canonical quadrature operators position $\hat{q} = \frac{1}{2}(\hat{a}^\dagger + \hat{a})$ and momentum $\hat{p} = \frac{i}{2}(\hat{a}^\dagger - \hat{a})$, satisfying the usual commutation relation $[\hat{p}, \hat{q}] = i$.

The cavity is coupled to the environment via short-time interactions with ancilla systems pumped in the cavity itself. Every ancilla η_k is a three-level lambda system. Its states are denoted by $|e\rangle$, $|g_1\rangle$, and $|g_2\rangle$, where $|e\rangle$ represents the excited state while $|e\rangle$, $|g_1\rangle$ are two ground states. In this basis, a thermal ancilla can be represented by the density operator

$$\eta_{th} = \begin{pmatrix} \alpha^2 & 0 & 0 \\ 0 & \frac{1}{2}\beta^2 & 0 \\ 0 & 0 & \frac{1}{2}\beta^2 \end{pmatrix} , \tag{4}$$

with the condition $|\alpha|^2 = 1 - |\beta|^2$ to have a unitary trace.

From such a thermal state, one can create coherences between ground levels, obtaining the coherent ancilla state which defines the so-called *phaseonium* [25]. Note that a little energy shift ϵ is created in the process. As seen in [26], we can assume that this shift is negligible and the ground-states

energy remains degenerate, writing the phaseonium density matrix as

$$\eta_k = \begin{pmatrix} \alpha^2 & 0 & 0 \\ 0 & \frac{\beta^2}{2} + \epsilon & \frac{\beta^2}{2} e^{-i\phi} \\ 0 & \frac{\beta^2}{2} e^{i\phi} & \frac{\beta^2}{2} - \epsilon \end{pmatrix} \approx \begin{pmatrix} \alpha^2 & 0 & 0 \\ 0 & \frac{\beta^2}{2} & \frac{\beta^2}{2} e^{-i\phi} \\ 0 & \frac{\beta^2}{2} e^{i\phi} & \frac{\beta^2}{2} \end{pmatrix}. \quad (5)$$

One can thus write a simple free Hamiltonian H_η for the phaseonium as

$$\hat{H}_\eta = \frac{\hbar\omega_\eta}{2}(\hat{\sigma}_1^+ \hat{\sigma}_1^- + \hat{\sigma}_2^+ \hat{\sigma}_2^-), \quad (6)$$

with ladder operators $\hat{\sigma}_i^\pm$ acting on the different ground levels of the ancilla

$$\begin{aligned} \hat{\sigma}_1^+ &= |e\rangle\langle g_1|, & \hat{\sigma}_1^- &= |g_1\rangle\langle e|, \\ \hat{\sigma}_2^+ &= |e\rangle\langle g_2|, & \hat{\sigma}_2^- &= |g_2\rangle\langle e|. \end{aligned} \quad (7)$$

Notice that the operators $\hat{\sigma}_i^\pm$ ($i = 1, 2$) refer to the ground state $|g_i\rangle$. We choose a resonant coupling with $\omega_c = \omega_\eta \equiv \omega$ and use the interaction picture to leave the free evolution of both cavity and bath out of the analysis. So, indicating with Ω the coupling strength, the total system-environment Hamiltonian at the k-th collision is given by the interaction term

$$\hat{V}_k = \hbar\Omega\left[\hat{a}(\hat{\sigma}_1^+ + \hat{\sigma}_2^+) + \hat{a}^\dagger(\hat{\sigma}_1^- + \hat{\sigma}_2^-)\right]. \quad (8)$$

IV. CAVITY-PHASEONIUM EVOLUTION

The time-evolution operator $\hat{U}_k = \exp(i\hat{V}_k\Delta t)$, with an arbitrary-long interaction time Δt, can be written in the basis of ancilla states $|e\rangle, |g_1\rangle, |g_2\rangle$, as (see Appendix A)

$$e^{-i\theta V_k} = \begin{pmatrix} \hat{C} & -iS^\dagger & -iS^\dagger \\ -i\hat{S} & \frac{1}{2}(\hat{C}' + \mathbb{I}) & \frac{1}{2}(\hat{C}' - \mathbb{I}) \\ -i\hat{S} & \frac{1}{2}(\hat{C}' - \mathbb{I}) & \frac{1}{2}(\hat{C}' + \mathbb{I}) \end{pmatrix}, \quad (9)$$

where θ is the accumulated Rabi phase $\hbar\Omega\Delta t$, while $\hat{C}, \hat{C}'$ and $\hat{S}$ are the photonic operators

$$\hat{C} = \cos(\theta\sqrt{2\hat{a}\hat{a}^\dagger}), \quad (10a)$$

$$\hat{C}' = \cos(\theta\sqrt{2\hat{a}^\dagger\hat{a}}), \quad (10b)$$

$$\hat{S} = \hat{a}^\dagger \frac{\sin(\theta\sqrt{2\hat{a}\hat{a}^\dagger})}{\sqrt{2\hat{a}\hat{a}^\dagger}}. \quad (10c)$$

Thanks to this representation, we are now able to write the map acting on the cavity at each step in its Kraus decomposition, which is

$$\rho_{k+1} = \mathcal{E}[\rho_k] = \mathrm{Tr}_k\left\{e^{-i\theta V_{k+1}} \rho_k \eta_{k+1} e^{i\theta V_{k+1}}\right\} = \sum_{i=0}^{4} \hat{E}_i \rho_k \hat{E}_i^\dagger, \quad (11)$$

with the operators $\hat{E}_i$ given by

$$\hat{E}_0 = \sqrt{\frac{\beta^2}{2}(1 - \cos\phi)}\,\mathbb{I}, \quad \hat{E}_1 = \sqrt{\frac{\gamma_\alpha}{2}}\,\hat{C}, \quad (12a)$$

$$\hat{E}_2 = \sqrt{\gamma_\alpha}\,\hat{S}, \quad \hat{E}_3 = \sqrt{\frac{\gamma_\beta}{2}}\,\hat{C}', \quad \hat{E}_4 = \sqrt{\gamma_\beta}\,\hat{S}^\dagger, \quad (12b)$$

where $\gamma_\alpha = 2\alpha^2$ and $\gamma_\beta = \beta^2(1 + \cos\phi)$.

Exploiting the relations $\hat{C}\hat{C} + 2\hat{S}^\dagger\hat{S} = \hat{C}'\hat{C}' + 2\hat{S}\hat{S}^\dagger = \mathbb{I}$, it is possible to write a finite difference master equation for the cavity alone at each interaction step, as

$$\Delta\rho_k = \sum_{i=0}^{4} \hat{E}_i \rho_k \hat{E}_i^\dagger - \rho_k = \sum_{i=1}^{4} \mathcal{D}[\hat{E}_i]\rho_k, \quad (13)$$

in which we adopt the usual definition for dissipator $\mathcal{D}[\hat{o}]\rho = \hat{o}\rho\hat{o}^\dagger - 1/2\{\hat{o}^\dagger\hat{o}, \rho\}$.

A. Cavity Steady State

Thanks to Eq. (13), the stationary state ρ^* of the system can be found solving the equation

$$\Delta\rho^* = 0. \quad (14)$$

The solution of the above equation (see Appendix C for details) can be expressed by the diagonal density matrix

$$\rho^* = \sum_{n}^{\infty} \frac{(\gamma_\alpha/\gamma_\beta)^n}{Z} |n\rangle\langle n|, \quad (15)$$

where $1/Z = \rho_{00}^*$ is the first element of the density matrix. We can then make a parallel with a standard Gibbs state [27] and set $(\gamma_\alpha/\gamma_\beta)^n = \exp(-n\hbar\omega/K_B T_\phi)$, where K_B is the Boltzmann constant, which defines an effective temperature T_ϕ

$$\exp\left\{\left(-\frac{\hbar\omega}{K_B T_\phi}\right)\right\} = \frac{\gamma_\alpha}{\gamma_\beta} \implies K_B T_\phi = -\hbar\omega/\ln\left(\frac{\gamma_\alpha}{\gamma_\beta}\right). \quad (16)$$

Since $\gamma_\alpha/\gamma_\beta = 2|\alpha|^2/(|\beta|^2(1 + \cos\phi))$, we emphasize that this effective temperature T_ϕ fundamentally depends on the coherence phase ϕ and on the excited-state population α of the phaseonium. Thus, *for every initial state* of the cavity in contact with the phaseonium beam, the system will end up in a thermal Gibbs state

$$\rho^* = \sum_{n}^{\infty} \frac{\exp(-E_n/K_B T_\phi)}{Z} |n\rangle\langle n|. \quad (17)$$

The above state is independent of the collision duration Δt, meaning that this is also the steady state of the continuous-limit master equation, as shown in Appendix B.

The range of temperatures spanned by ancilla parameters α and ϕ is shown in Figure 2. Seeing that temperature is positive-defined, our Gibbs state representation works as long as we have low-excited ancilla probability such that $\gamma_\alpha/\gamma_\beta <$
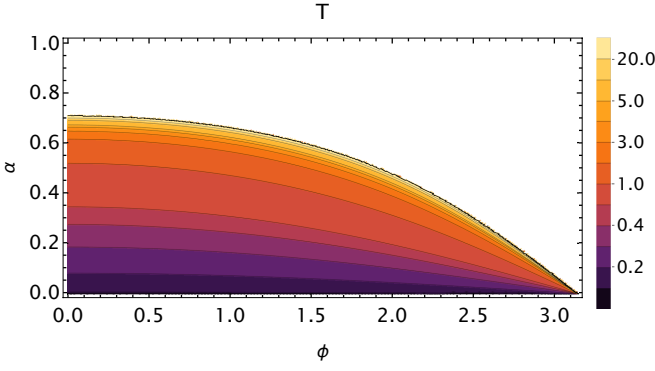
FIG. 2. Range of steady-state temperatures of one cavity in contact with a phaseonium bath, as a function of excited-state population α and ground-state coherences ϕ of phaseonium atoms. Temperature is symmetric in ϕ, so it is shown in the range $0 \le \alpha \le 1$, $0 \le \phi \le \pi$.

1. Two special cases emerge: (i) when $|\alpha|^2 = 0$, the system depletes itself and ends up in a vacuum thermal state (the atoms only absorb photons from the cavity radiation field); (ii) when $|\alpha|^2 = |\beta|^2 \cos^2(\phi/2)$, that is $\gamma_\alpha/\gamma_\beta = 1$, Eq. (16) does not hold, leading to an infinite temperature. Thus, for $\gamma_\alpha/\gamma_\beta \ge 1$ this description is no more accurate and we can conclude that, under these conditions, the hypothesis of Eq. (14) of the existence of a stationary state is no more valid. Also, the value $\phi = \pi$ is to be excluded, since it makes the ratio $\gamma_\alpha/\gamma_\beta$ undefined.

Since we have not specified the initial state of the system, we can infer that this fixed point state ρ^* of the collision map is unique and reached whatever the initial state of the system.

The final thermalization temperature T_ϕ of the cavity is in general different from the temperature T of the starting thermal ancillas η_{th} defined in Eq. (4), before the ground-state coherences are created. Indeed, there is an energetic cost in creating quantum coherences. This energy difference can be expressed by

$$\frac{\hbar\omega}{K_B T_\phi} - \frac{\hbar\omega}{K_B T} = \ln(1 + \cos(\phi)). \tag{18}$$

Assuming that between the system and the phaseonium atoms there is only heat exchange, it is possible to define an *apparent* temperature $\mathcal{T}$ even if the atoms are not in a thermal state [28, 29]. This apparent temperature is defined as

$$K_B\mathcal{T} = \hbar\omega \left[\ln\left(\frac{\text{Tr}_S\left\{ (\hat{\sigma}_1^+ + \hat{\sigma}_2^+)(\hat{\sigma}_1^- + \hat{\sigma}_2^-)\eta_k \right\}}{\text{Tr}_S\left\{ (\hat{\sigma}_1^- + \hat{\sigma}_2^-)(\hat{\sigma}_1^+ + \hat{\sigma}_2^+)\eta_k \right\}} \right) \right]^{-1}, \tag{19}$$

where $\hat{\sigma}_i^\pm$ are the atomic operators of the three-level ancillas defined in Eq. (7). Remarkably, it can be shown that this coincides with the expression of the stationary effective temperature of the system T_ϕ given in Eq. (16).

B. Ancilla Steady State

Thanks to the above result, we can also retrieve the ancilla's stationary state once the cavity has thermalized. Using

Eqs. (17) and (9), and performing the partial trace over the system degrees of freedom, we obtain

$$\eta^{\text{st}} = \text{Tr}_S\left\{ \hat{U}_k \rho^* \eta_k \hat{U}_k \right\} = \begin{pmatrix} |\alpha|^2 & 0 & 0 \\ 0 & \frac{|\beta|^2}{2} & \frac{|\beta|^2}{2}\Gamma^\dagger \\ 0 & \frac{|\beta|^2}{2}\Gamma & \frac{|\beta|^2}{2} \end{pmatrix}, \tag{20}$$

where $\Gamma = \cos(\phi) - i\sin(\phi)\,\text{Tr}\{\hat{C}'\rho^*\}$. Note that for finite collision time the stationary ancilla's coherences are modified by the interaction with the cavity, but taking the continuous time limit this not hold any more. Indeed, in the latter limit, we have $\text{Tr}\{\hat{C}'\rho^*\} \sim \text{Tr}\{(\mathbb{I} - \hat{a}^\dagger\hat{a}\theta^2)\rho^*\}$ (see Appendix B).

We stress that this evolved ancilla carries the same steady-state system temperature, given only by the real part of coherences, as in Figure 2. Ancillas can thus be exploited again to let another cavity thermalize at the same temperature. We shall investigate this situation in the following sections.

V. CASCADE CAVITY-PHASEONIUM EVOLUTION

We now take a system of two identical single-mode cavities, S_1, S_2, subject to the same collision interaction with a beam of phaseonium atoms (see Figure 1). They are arranged in a way that every ancilla atom first interacts with the subsystem S_1, modifying it, and successively with the second subsystem S_2. This is called *cascade quantum system* [30].

We must consider the total evolution of the bipartite system S made of the two cavities S_1 and S_2. This translates in the subsequent application of unitary interaction operators $\hat{U}_{j,k}$ ($j = 1, 2$ corresponds to the cavity S_j) to the overall density operator of both system and ancilla. Indicating with ρ_k and η_k, respectively, the density operators of the two-cavity system S and of the ancilla atom at the k-th interaction step, extending Eq. (2) we have

$$\rho_k = \mathcal{E}[\rho_{k-1}] = \text{Tr}_k\left\{ \hat{U}_{2,k}\hat{U}_{1,k}\rho_{k-1} \otimes \eta_k \hat{U}_{1,k}^\dagger \hat{U}_{2,k}^\dagger \right\}. \tag{21}$$

The crucial property of such dynamics relies on the fact that cavity S_1 "does not see" the following cavity S_2, so that its evolution is again described by Eq. (11). S_1 interacts only with ancillas in their initial state η_k. After that interaction, however, the ancilla state is modified. The dynamics of subsystem S_2 thus depend on that of subsystem S_1. By the action of common ancilla atoms, the two subsystems get correlated. This is explained by the fact that the common phaseonium ancilla atoms mediate the interaction between the cavity subsystems. If we trace out S_1 from Eq. (21), we get the state of the cavity S_2 alone as

$$\begin{aligned} \rho_{2,k} &= \text{Tr}_{S_1}\left\{ \text{Tr}_k\left\{ \hat{U}_{2,k}\hat{U}_{1,k}(\rho_{k-1} \otimes \eta_k)\hat{U}_{1,k}^\dagger\hat{U}_{2,k}^\dagger \right\} \right\} \\ &= \text{Tr}_k\left\{ \hat{U}_{2,k}\,\text{Tr}_{S_1}\left\{ \hat{U}_{1,k}(\rho_{k-1} \otimes \eta_k)\hat{U}_{1,k}^\dagger \right\} \hat{U}_{2,k}^\dagger \right\}. \end{aligned} \tag{22}$$

Cavity S_2 does not follow a Completely Positive Trace Preserving (CPT) map and its dynamics is non-Markovian.

Following an analogous analysis of that of Section IV, it can be shown that the map of the two-cavity system S is represented by the Kraus operators

$$\hat{E}_0 = \sqrt{\frac{\beta^2}{2}(1-\cos\phi)}\,\mathbb{I}\,, \tag{23a}$$

$$\hat{E}_1 = \sqrt{\frac{\gamma_\alpha}{2}}\,(\hat{C}\otimes\hat{C}-2\hat{S}\otimes\hat{S}^\dagger)\,, \tag{23b}$$

$$\hat{E}_2 = \sqrt{\gamma_\alpha}\,(\hat{S}\otimes\hat{C}'+\hat{C}\otimes\hat{S})\,, \tag{23c}$$

$$\hat{E}_3 = \sqrt{\gamma_\beta}\,(\hat{S}^\dagger\otimes\hat{C}+\hat{C}'\otimes\hat{S}^\dagger)\,, \tag{23d}$$

$$\hat{E}_4 = \sqrt{\frac{\gamma_\beta}{2}}\,(\hat{C}'\otimes C'-2\hat{S}^\dagger\otimes\hat{S})\,. \tag{23e}$$

With these operators, we can finally determine the finite difference master equation for the evolution of the two-cavity system S

$$\Delta\rho_k = \sum_{i=1}^{4}\mathcal{D}\left[\hat{E}_i\right]\rho_k\,. \tag{24}$$

VI. APPLICATION

Having found the master equation of Eq. (24), we can follow the evolution of the two cavity fields while interacting with the beam of phaseonium atoms. As we have seen, this is a thermalization process. In this section we provide an application of this controlled process which leads to heating and cooling the cavities.

Let us summarize in a simple protocol how to exploit the model we developed so far:

1. Choose a temperature T^* and pick a pair of parameters $\{\alpha^*, \phi^*\}$ from Fig. 2 corresponding to that temperature, or use Eq. (16) to find them;

2. Prepare an ensemble of three-level lambda thermal atoms characterized by an excited-state population α^*;

3. Split the degenerate ground doublet of those atoms by creating a certain amount of coherence characterized by the phase ϕ^*—now you have an ensemble of phaseonium atoms;

4. Inject a beam of phaseonium atoms one at a time, inside the two cavities, placed in a cascade configuration, so that the atoms interact with each cavity for a time Δt^*;

5. After some time, the temperature of each cavity will be the initially chosen temperature T^*.

Recall that, in general, this temperature will be *different* from that of the initially prepared thermal ancillas at step 2, due to the energetic cost of creating quantum coherences in the atomic state.

With this protocol in mind, we show in the following some results about the exploitation of phaseonium atoms to drive the dynamics of the two cavity fields towards desired target states.
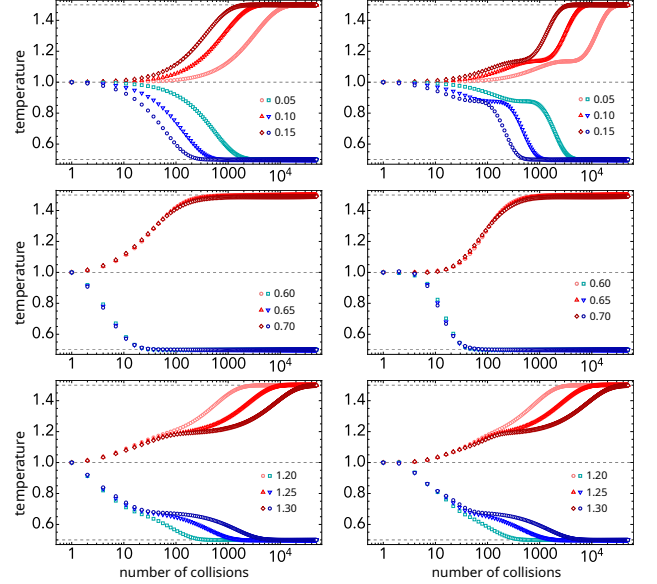

FIG. 3. Behaviour of temperature of the first cavity (left column) and second cavity (right column) taking different values for the collision time. The initial state of both the subsystems is taken to be a thermal state at $T = 1$. In each plot is shown the thermalization process obtained involving ancillas with a different amount of coherences (but the same $\alpha=0.25$). More precisely, for the hot curves $\phi = 1.5855$ and for the cold curves $\phi = 2.4043$, that correspond to stationary temperatures for the cavities $T = 1.5$ and $T = 0.5$, respectively. We observe as increasing the collision time the thermalization process becomes faster for small Δt, does not change for $\Delta t \sim 0.6$ and becomes slower for $\Delta t > 1.2$.

A. Heating and Cooling the Cavities

Firstly, we demonstrate how general the protocol is: choosing any temperature T^*, one can always find a pair of phaseonium parameters to heath up as well as cool down the cavities towards that temperature.

In Figure 3 we show that for a fixed excited-state population α, gauging the coherence phase ϕ, we can actually control the evolution of the system to make it getting hotter or colder. In particular, it is seen how, starting from a thermal state at $T = 1.0$ for both cavities, we can appropriately choose the values of the phase ϕ such that the two subsystems thermalize either to a temperature $T = 1.5$ or to $T = 0.5$. We notice how cavity S_1 is always the first to thermalize: this is clear given the unidirectionality of the cascade two-cavity system. The second cavity S_2 eventually reaches the same stable temperature of S_1. Regarding the speed of the thermalization process, it depends on all three parameters, α, ϕ and Δt. Having already prepared our phaseonium atoms, we can then easily change the interaction time to speedup or slow down the process.

As displayed in the three rows of Figure 3, the behaviour of the thermalization as a function of the number of collisions depends on the atom-cavity interaction time Δt, but in each row this dependence is different: for interaction times of the order of 0.10 the process speeds up by increasing Δt (panels in
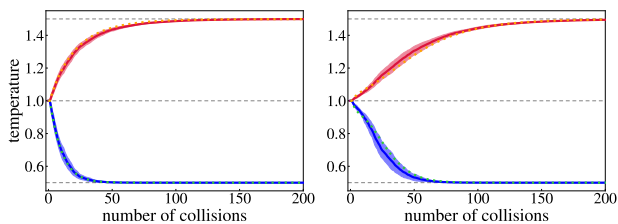
FIG. 4. Behaviour of the temperature of the first cavity S_1 (right panel) and second cavity S_2 (left panel) using interaction times extracted at every step k from a Gaussian distribution: $\Delta t_k = (0.4 \pm 0.2)$, where the standard deviation is used as the error on the mean. Here we selected $\phi^* = \pi/2$, and for the hot curves we use $\alpha^* = 0.2517517$, corresponding to a stationary temperature $T^* = 1.5$, while for the cold curves we have $\alpha^* = 0.451963$, corresponding to a stationary temperature $T^* = 0.5$. The mean value across ten simulations of the evolving temperature is plotted as a continuous line, surrounded by its standard deviation. For reference, the constant interaction time case with $\Delta t_k = 0.4$ is plotted with a dotted line. It is evident that both heating and cooling the cavities with noise in the interaction times slows down the thermalization process, although the final stable temperature is reached at some point.

the top row); for interaction times of the order of 1.25 the process slows down by increasing Δt (panels in the bottom row); for intermediate interaction times the change in speed is negligible (panels in the central row). This alternating behaviour can be understood remembering that the interaction time Δt appears in the time evolution of the system of Eq. (24) only inside the sinusoidal operators given in Eq. (10).

B. Robustness of the Model

Here we address the real-world scenario where our parameters, particularly ϕ and Δt are affected by stochastic noise, so they are not constant but belong to some stochastic distribution. In fact, suppose a velocity selector is placed in front of the phaseonium beam. As illustrated in Figure 1, the time each atom spends in a cavity gives the interaction time Δt, and so it depends on the selected velocity of phaseonium atoms. We can consider the selector to be flawed and characterized by an absolute error on selected speeds, and those to be Gaussian distributed. Interaction times will then follow the same distribution, with a variable $\Delta t \equiv \Delta t_k$ changing at each interaction step k. Similarly, in the creation of phaseonium atoms of Eq. (5), the coherence phase ϕ of each atom can be considered as a stochastic Gaussian variable $\phi \equiv \phi_k$, centred on the target coherence phase ϕ^*. We then expect a thermalization process for both cavities that takes them to a stochastic temperature $T^* \pm \Delta T^*$. We will confront this temperature T^* with the expected temperature T_{ϕ^*} given by the mean value of the prepared atom coherences.

Thanks to the Markovianity of our approach, where every interaction is independent of the others and the stroboscopic evolution is calculated step-by-step, it is well suited to tackle the problem of stochastic parameters: we can always apply
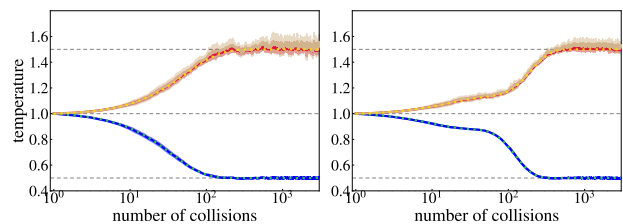

FIG. 5. Behaviour of the temperature of the first cavity S_1 (right panel) and second cavity S_2 (left panel) using coherence phases ϕ_k extracted at every step k from a Gaussian distribution with standard deviation σ. For the cooling process, we select $\alpha^* = 0.25$ and $\phi_k^* = 1.585589386$, with $\sigma = 0.2$, corresponding to a stationary temperature $T^* = 0.5$. For the heating process, we have two simulations with increasing standard deviation, using $\alpha^* = 0.5$ and $\phi_k^* = 1.26768686$, with $\sigma = 0.2$ for the red curve and $\sigma = 0.35$ for the brown curve, both corresponding to a stationary temperature $T^* = 1.5$. Interaction time $\Delta t_k = 0.2$ is fixed. The mean value across ten simulations of the evolving temperature is plotted as a continuous line, surrounded by its standard deviation across different simulations. For reference, the constant coherence case with $\sigma = 0$ is plotted with a dotted line. The cooling process is not much affected by random variations in the coherence phase: the first cavity reaches a noisy stable state at $T_1 = (0.498 \pm 0.006)$, and the second thermalizes at $T_2 = (0.498 \pm 0.004)$. Noise is higher in the heating scenario, with $T_1 = (1.50 \pm 0.03)$ and $T_2 = (1.50 \pm 0.02)$ for the red curve with $\sigma = 0.2$ and $T_1 = (1.52 \pm 0.05)$ and $T_2 = (1.52 \pm 0.03)$ for the brown curve with $\sigma = 0.35$.

Eq. (24) to each evolution step k, using each time the corresponding Δt_k and ϕ_k.

The effect of the noisy interaction times is not expected to significantly affect the thermalization process, since the final temperature of Eq. (16) does not depend on this parameter: no matter the interaction time, every collision will take the system closer to the final stable temperature. This can be seen from the simulations in Figure 4, which shows two thermalization processes for the two cavities from initial temperature $T = 1.0$ to temperatures $T_{\phi^*} = 1.5$ and $T_{\phi^*} = 0.5$, where ϕ_k is fixed to ϕ^*. The reference cases with constant Δt_k are represented with dotted line. For the stochastic Δt_k cases, we report with a continuous line the mean values across different simulations, surrounded by a halo representing the standard deviation.

Different is the case with stochastic coherence phases ϕ_k and fixed interaction time $\Delta t_k = \Delta t$, shown in Figure 5 and Figure 6 in the same fashion as the previous figure. In Figure 5 we can see that cooling to temperature $T_{\phi^*} = 0.5$ presents only little noise in the final stable temperature, while the heating scenario suffers more, showing manifest noise around the mean value but still getting to an average steady temperature close to the predicted $T_{\phi^*} = 1.5$. Moreover, as can be seen from the two heating processes plotted, the precision of heating is affected by the precision in preparing phaseonium atoms. Figure 6 shows different and non-trivial behaviour: heating and cooling with stochastic coherence phases drawn from a different region of the parameter landscape in Figure 2 lead to a steady-state temperature T^* for both cavities which is
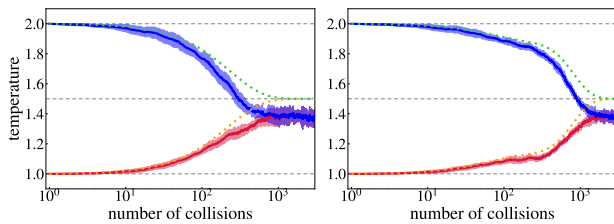
FIG. 6. Behaviour of the temperature of the first cavity S_1 (right panel) and second cavity S_2 (left panel) using coherence phases ϕ_k extracted at every step k from a Gaussian distribution with standard deviation $\sigma = 0.2$. Here we selected the same set of parameters $\alpha^* = 0.25$ and $\phi_k^* = (2.404315987 \pm 0.2)$, corresponding to a stationary temperature $T^* = 1.5$, but with two different initial conditions for the cavities: starting at temperatures $T_0 = 2.0$ or $T_0 = 1.0$. Interaction time $\Delta t_k = 0.2$ is fixed. The mean value across ten simulations of the evolving temperature is plotted as a continuous line, surrounded by its standard deviation. For reference, the constant coherence case with $\phi_k = 2.404315987$ and $\phi_k = 1.585589386$ is plotted with a dotted line. A clear difference arises in the reference thermalization at $T^* = 1.5$ and the two stochastic processes. In fact, in both cases, the first cavity thermalizes to a noisy temperature $T_1 = (1.37 \pm 0.04)$ and the second to $T_2 = (1.37 \pm 0.03)$.

lower than the expected temperature T_{ϕ^*}. This can be understood looking at the resulting stochastic distribution of ancillas' apparent temperatures defined in Eq. (19). In fact, given the nonlinear behaviour of the temperature in ϕ, the resulting distribution will be right-skewed. This will shift the mode to the left of the mean, so that we are really sending through the cavities a bigger number of "cooler" ancillas with temperature $T_k < T_{\phi^*}$, lowering the final temperature of the systems.

VII. DISCUSSION

In this paper, we have studied the dynamics of two optical cavities immersed in a phaseonium bath, highlighting how the quantum coherence present in the initial state of this peculiar atomic environment affects the cavity evolved state. In particular, the two-cavity system, assembled in a cascade configuration, thermalizes at a temperature T_ϕ which depends on the coherence between the ground levels of the phaseonium. We have found the quantum dynamical map (see Eq. (24)) for finite interaction times using only few assumptions required by collision models. In general, this equation can be used to calculate the evolution of observables on the system via Eq. (D3).

It is also possible to see the unidirectionality of the cascade: the first cavity evolves independently of the second cavity, following the dynamical map of Eq. (13), and it is the first to reach the steady state given by Eq. (17). From this moment on, every subsequent ancilla is altered in the same way by the previous interaction and ends up in the state of Eq. (20). This state then makes the second cavity to thermalize at the same temperature T_ϕ of the first cavity.

Remarkably, we have demonstrated that, by suitably harnessing excited-state population and coherence phase of each phaseonium atom, the cavity fields can be heated up or cooled

down with respect to their initial temperature.

From an experimental point of view, the use of two harmonic oscillators (here represented by single-mode cavities) and Gaussian states allows us to work with general-purpose systems that are easy to implement in various ways. Preparation of phaseonium atoms is also possible via stimulated Raman adiabatic passage (STIRAP) [31, 32], or similarly fractional STIRAP [33] or fractional Stark-chirped rapid adiabatic passage (f-SCRAP) [34], Morris-Shore transformation [35], or quantum Householder reflection [36]. Thermodynamic cost of create phaseonium atoms is studied in [26].

Finally, from given dynamical equations, it is straightforward to take the continuous limit for $\Delta t \to 0$, but we emphasize that in real implementations the interaction time is finite and can be used as control parameters. The time spent by an ancilla inside the cavity can be easily set by a velocity selector for phaseonium atoms.

These results open the way to various prospects. Future works will investigate the role of intra system quantum correlations, created by the ancillas interacting with both cavities. In fact, although the cavities are not directly coupled with each other, a unidirectional flow of information is mediated by the ancilla atoms, going from the first cavity to the second one. Working with quadratic operators like we did in Appendix B, approximating the time-evolution operator for small collision times, one can exploit the theory of continuous systems' covariance matrices as a useful tool for looking at the evolution of the von Neumann entropy, exchanged mutual information [37, 38], quantum discord [39–42], and even entanglement via logarithmic negativity as an entanglement monotone [43–45]. The starting point for this further studies is given in Appendix D. Moreover, another interesting direction to be analysed is the utilization of different types of ancilla phaseonium atoms, prepared with different coherences, to induce a thermodynamic cycle on the cavities.

Appendix A: Time-Evolution Operator Expansion

This appendix contains the key passages to recover a manageable expression of the evolution operator $\hat{U}_k$ that rules the evolution of the system $\rho_{k-1} \otimes \eta_k$ and will lead us to the Kraus map 12. This operator is naturally given by the exponential of the cavity-ancilla interaction 8, $\hat{U}_k = \exp\{-i\Delta t \hat{V}_k\}$. We can collect the interaction strength $\hbar\Omega$ outside the interaction Hamiltonian and call $\hbar\Omega\Delta t$ as the accumulated Rabi phase θ during the interaction. Therefore, we can expand the unitary

evolution operator $\hat{U}_k = exp(i\theta\hat{V}_k)$ as

Hamiltonian in the ancilla basis $|e\rangle, |g_1\rangle, |g_2\rangle$, that is

$$\hat{V}_k = \begin{pmatrix} 0 & \hat{a} & \hat{a} \\ \hat{a}^\dagger & 0 & 0 \\ \hat{a}^\dagger & 0 & 0 \end{pmatrix}. \tag{A2}$$

By brute matrix multiplication we can calculate $\hat{V}_k^2$ and $\hat{V}_k^3$, and easily infer a rule for even and odd powers, as we will show later. Now the summation in Eq. (A1) is to be intended matrix element by matrix element.

$$e^{i\theta\hat{V}_k} = \sum_{j=0}^{\infty} \frac{(i\theta)^j}{j!} V_k^j = \mathbb{I} + \sum_{j=1}^{\infty} \frac{(i\theta)^{2j}}{(2j)!} V_k^{2j} + \sum_{j=1}^{\infty} \frac{(i\theta)^{2j-1}}{(2j-1)!} V_k^{2j-1} \tag{A1}$$

We will see shortly why this decomposition in even and odd powers is convenient, but first we must reframe the interaction

Referring each element of $\hat{U}_k$ in row r and columns l as $\hat{U}_k^{(rl)}$, we can sum up again each series and recover the three by three time-evolution operator $\hat{U}_k$ given in Eq. (9).

One finds that the rules for even and odd powers of $\hat{V}_k$ are:

$$V_k^{2j} = \begin{pmatrix} 2^i(\hat{a}\hat{a}^\dagger)^j & 0 & 0 \\ 0 & 2^{j-1}(\hat{a}^\dagger\hat{a})^j & 2^{j-1}(\hat{a}^\dagger\hat{a})^j \\ 0 & 2^{j-1}(\hat{a}^\dagger\hat{a})^j & 2^{j-1}(\hat{a}^\dagger\hat{a})^j \end{pmatrix}, \tag{A3}$$

$$V_k^{2j-1} = \begin{pmatrix} 0 & 2^{j-1}(\hat{a}\hat{a}^\dagger)^{j-1}\hat{a} & 2^{j-1}(\hat{a}\hat{a}^\dagger)^{j-1}\hat{a} \\ 2^{j-1}(\hat{a}^\dagger\hat{a})^{j-1}\hat{a}^\dagger & 0 & 0 \\ 2^{j-1}(\hat{a}^\dagger\hat{a})^{j-1}\hat{a}^\dagger & 0 & 0 \end{pmatrix}. \tag{A4}$$

For even powers of the time-evolution operator expansion we have the elements:

$$\hat{U}_k^{(11)} = \sum_{j=1}^{\infty} \frac{(i\theta)^{2j}}{(2j)!} 2^k(\hat{a}\hat{a}^\dagger)^j = \sum_{j=1}^{\infty}(-1)^j \frac{\theta^{2j}(\sqrt{2\hat{a}\hat{a}^\dagger})^{2j}}{(2j)!} = \cos\left(\theta\sqrt{2\hat{a}\hat{a}^\dagger}\right) - \mathbb{I}, \tag{A5}$$

$$\hat{U}_k^{(22)} = \hat{U}_k^{(23)} = \hat{U}_k^{(32)} = \hat{U}_k^{(33)} = \sum_{j=1}^{\infty} \frac{(i\theta)^{2j}}{(2j)!} 2^{j-1}(\hat{a}^\dagger\hat{a})^j = \frac{1}{2}\sum_{j=1}^{\infty}(-1)^j \frac{\theta^{2j}(\sqrt{2\hat{a}^\dagger\hat{a}})^{2j}}{(2j)!} = \frac{1}{2}\left[\cos\left(\theta\sqrt{2\hat{a}^\dagger\hat{a}}\right) - \mathbb{I}\right], \tag{A6}$$

and for odd powers we have the elements:

$$\hat{U}_k^{(12)} = \hat{U}_k^{(13)} = \sum_{j=1}^{\infty} \frac{(i\theta)^{2j-1}}{(2j-1)!} 2^{j-1}\hat{a}^\dagger(\hat{a}\hat{a}^\dagger)^{j-1} = \sum_{j=1}^{\infty}(-1)^j\hat{a}^\dagger \frac{\theta^{2j-1}(\sqrt{2\hat{a}\hat{a}^\dagger})^{jk-1}}{(2j-1)!\sqrt{2\hat{a}\hat{a}^\dagger}} = i\hat{a}^\dagger \frac{\sin\left(\theta\sqrt{2\hat{a}\hat{a}^\dagger}\right)}{\sqrt{2\hat{a}\hat{a}^\dagger}}, \tag{A7}$$

$$\hat{U}_k^{(21)} = \hat{U}_k^{(31)} = \sum_{k=1}^{\infty} \frac{(i\theta)^{2j-1}}{(2j-1)!} 2^{j-1}(\hat{a}\hat{a}^\dagger)^{k-1}\hat{a} = i\sum_{j=1}^{\infty}(-1)^j \frac{\theta^{2j-1}(\sqrt{2\hat{a}\hat{a}^\dagger})^{2j-1}}{(2j-1)!\sqrt{2\hat{a}\hat{a}^\dagger}}\hat{a} = i\frac{\sin\left(\theta\sqrt{2\hat{a}\hat{a}^\dagger}\right)}{\sqrt{2\hat{a}\hat{a}^\dagger}}\hat{a}, \tag{A8}$$

having used in the first line the equivalence $f(\hat{a}^\dagger\hat{a})\hat{a}^\dagger = \hat{a}^\dagger f(\hat{a}\hat{a}^\dagger)$.

We can thus define the photon operators that appear in the elements of the time-evolution operator as in eq. (10), and with those we can rewrite the exponential operator in terms of the 3×3 matrix representation in the ancilla's basis

$$e^{-i\theta\hat{V}_k} = \begin{pmatrix} \hat{C} & -iS^\dagger & -iS^\dagger \\ -i\hat{S} & \frac{1}{2}(\hat{C}' + \mathbb{I}) & \frac{1}{2}(\hat{C}' - \mathbb{I}) \\ -i\hat{S} & \frac{1}{2}(\hat{C}' - \mathbb{I}) & \frac{1}{2}(\hat{C}' + \mathbb{I}) \end{pmatrix}. \tag{A9}$$

Note that now the time-dependence of the evolution is hidden inside the sinusoidal functions of photon operators $\hat{C}, \hat{C}'$ and $\hat{S}$.

Appendix B: Continuous Time Limit

We show here the continuous time limit of the master equation 13 for the cascade system. Revising Ref. [8], continuous time is a standard approximation in collision models approaches, where system-ancilla interactions are taken to be short enough to allow a second-order approximation of the time-evolution operator $\hat{U}_k$. As long as collisions *must happen*, the limit $\Delta t \to 0$ can survive only for diverging interaction strengths; else, one focus on evolution times much larger than Δt, so that the stroboscopic dynamics happening at discrete time steps $t_n = n\Delta t$ can be replaced with a continuous time variable t, and finite differences can be replaced with differentials. This is called *coarse graining*. In this approxima-

tion, photonic operators in eq. (10) become

$$C = \mathbb{I} - \theta^2 aa^\dagger \qquad C' = \mathbb{I} - \theta^2 a^\dagger a \qquad S = \theta a^\dagger \qquad \text{(B1)}$$

and denoting $\hat{a}$ ($\hat{a}^\dagger$) and $\hat{b}$ ($\hat{b}^\dagger$) as the annihilation (creation) operators for the first and second cavity respectively, the Kraus operators in eq. (23) can be written as

$$E_0 = \sqrt{1 - \frac{\gamma_\alpha}{2} - \frac{\gamma_\beta}{2}}\,\mathbb{I}, \qquad \text{(B2)}$$

$$E_1 = \sqrt{\frac{\gamma_\alpha}{2}}\left[1 - \theta^2\hat{b}\hat{b}^\dagger - \theta^2\hat{a}\hat{a}^\dagger - 2\theta^2\hat{a}^\dagger\hat{b}\right], \qquad \text{(B3)}$$

$$E_2 = \sqrt{\gamma_\alpha}\left[\theta\hat{a}^\dagger + \theta\hat{b}^\dagger\right], \qquad \text{(B4)}$$

$$E_3 = \sqrt{\gamma_\beta}\left[\theta\hat{a} + \theta\hat{b}\right], \qquad \text{(B5)}$$

$$E_4 = \sqrt{\frac{\gamma_\beta}{2}}\left[1 - \theta^2\hat{b}^\dagger\hat{b} - \theta^2\hat{a}^\dagger\hat{a} - 2\theta^2\hat{a}\hat{b}^\dagger\right], \qquad \text{(B6)}$$

We can now use these expressions to rewrite the discrete master equation (13) as

$$\left[\frac{\gamma_\alpha}{2}\sin^2\theta\sqrt{2n}\right]\rho_{n-1}^{*n-1} + \left[\frac{\gamma_\alpha}{2}\cos^2\theta\sqrt{2(n+1)} + \frac{\gamma_\beta}{2}\cos^2\theta\sqrt{2n} + \frac{\beta^2}{2}(1-\cos\phi)\right]\rho_n^{*n} + \left[\frac{\gamma_\beta}{2}\sin^2\theta\sqrt{2(n+1)}\right]\rho_{n+1}^{*n+1} = \rho_n^{*n} \quad \text{(C3)}$$

This can be recursively resolved obtaining

$$\rho_n^{*n} = \frac{\gamma_\alpha}{\gamma_\beta}\rho_{n-1}^{*n-1} = \left(\frac{\gamma_\alpha}{\gamma_\beta}\right)^n\rho_0^{*0}. \qquad \text{(C4)}$$

We can now set ρ_0^{*0} as $1/Z$ and $\left(\gamma_\alpha/\gamma_\beta\right)^n = \exp\left(-n\hbar\omega/K_BT_\phi\right)$ to write the steady state as a Gibbs State:

$$\rho^* = \sum_n^\infty \frac{\exp\left(-E_n/K_BT_\phi\right)}{Z}|n\rangle\langle n|. \qquad \text{(C5)}$$

and thus define the steady state phase-dependent temperature T_ϕ given in 16.

As the first cavity thermalizes to this temperature, ancillas will cease to interact with it and the second cavity will start to see the originally prepared ancillas bearing the same T_ϕ and to evolve like it was a single cavity, finally thermalizing to T_ϕ.

Since this derivation of the steady state is the most general, it will hold as for the coarse-grained dynamics expressed by Eq. (B7). The steady state temperature, in fact, does not depend on the interaction time Δt.

$$\frac{d\rho(t)}{dt} = -i[\hat{H}_{\text{eff}},\rho] + \gamma'_\alpha\,\mathcal{D}[\hat{a}^\dagger{+}\hat{b}^\dagger]\hat{\rho}(t) + \gamma'_\beta\,\mathcal{D}[\hat{a}{+}\hat{b}]\hat{\rho}(t) \qquad \text{(B7)}$$

where $\hat{H}_{\text{eff}} = i(\gamma'_\beta - \gamma'_\alpha)(\hat{a}^\dagger\hat{b} - \hat{b}^\dagger\hat{a})/2$ and $\gamma'_{\alpha,\beta} = \gamma_{\alpha,\beta}\Omega^2\Delta t$, considering always Ω such that $\Omega^2\Delta t$ converges in the continuous limit. This cascade master equation is comparable to that obtained by the standard collision model methods explained in [8].

Appendix C: Cavity Steady State

Here we look for the steady state of one cavity after a *sufficient* number of collisions. The stationary condition reads

$$\Delta\rho^* = \sum_i \hat{E}_i\rho^*\hat{E}_i^\dagger - \rho^* = 0. \qquad \text{(C1)}$$

with Kraus operators given in Eq. (12). This must be true for each expectation value in the system's basis, so using the relations $f(\hat{a}\hat{a}^\dagger)|n\rangle = f(n+1)|n\rangle$ and $f(\hat{a}^\dagger\hat{a})|n\rangle = f(n)|n\rangle$ we have that off-diagonal elements are null,

$$\Delta\rho_m^{*n} \equiv \langle n|\Delta\rho^*|m\rangle = 0, \qquad \text{(C2)}$$

and for $n = m$ we report the relative equation

Appendix D: Operators Evolution

The variation of the expectation value of an observable acting on the Hilbert space of the system in each collision is given by, cf. eq. (13):

$$\text{Tr}\{\hat{O}\,\Delta\rho_k\} = \text{Tr}\left\{\hat{O}\left(\sum_{i=0}^4\hat{E}_i\rho_k\hat{E}_i^\dagger - \rho_k\right)\right\} \qquad \text{(D1)}$$

Thanks the permutation property of the trace, this can be recast into

$$\text{Tr}\left\{\left(\sum_{i=0}^4\hat{E}_i^\dagger\hat{O}\hat{E}_i - \hat{O}\right)\rho_k\right\} = \text{Tr}\{\Delta\hat{O}\,\rho_k\} \qquad \text{(D2)}$$

leading to the following discrete master equation for $\langle\hat{O}\rangle_k$

$$\Delta\langle\hat{O}\rangle_k = \sum_{i=1}^4\langle\widetilde{\mathcal{D}}[E_i]\hat{O}\rangle_k \qquad \text{(D3)}$$

where $\widetilde{\mathcal{D}}[\hat{E}]\hat{O} = \hat{E}^\dagger \hat{O}\hat{E} - 1/2\{\hat{E}^\dagger \hat{E}, \hat{O}\}$. Taking the continuous time limit as in Eq. (B7), we obtain

$$\frac{d\langle \hat{O}\rangle}{dt} = \langle i[\hat{H}_{\text{eff}}, \rho]\rangle + \gamma'_\alpha \langle \widetilde{\mathcal{D}}[\hat{a}^\dagger + \hat{b}^\dagger]\,\hat{O}\rangle + \gamma'_\beta \langle \widetilde{\mathcal{D}}[\hat{a} + \hat{b}]\,\hat{O}\rangle$$

(D4)

We emphasize a crucial distinction from eq. (D3): the presented master equation is quadratic in the cavity operators, thereby preserving Gaussianity. Consequently, the utility of working with Gaussian states becomes evident. Gaussian states, when subjected to such a coarse-grained quantum map, undergo evolution while retaining their Gaussian nature. As a result, the density matrix ρ_k manifests as a bipartite Gaussian state with two modes. Its characterization involves the expectation values of the vector $\vec{r} = (\hat{q}_1, \hat{p}_1, \hat{q}_2, \hat{p}_2)$ and the covariance matrix $\boldsymbol{\Sigma} = \left\langle \frac{1}{2}(\hat{r}_m \hat{r}_n + \hat{r}_n \hat{r}_m)\right\rangle - \langle \hat{r}_m\rangle\langle \hat{r}_n\rangle$, where $m, n = 1, \ldots, 4$. Furthermore, it is noteworthy that states with $\langle \vec{r}\rangle = 0$ can always be selected. This implies that the system's characterization at each stage of evolution is entirely captured only by the second moments.

[1] M. O. Scully, Phys. Rep. **219**, 191 (1992).

[2] M. O. Scully and S. Zhu, in *Foundations of Quantum Mechanics* (World Scientific, 1992) pp. 335–341.

[3] M. O. Scully, M. S. Zubairy, G. S. Agarwal, and H. Walther, Science **299**, 862 (2003).

[4] U. Rathea, M. Fleischhauer, and M. O. Scully, in *Frontiers in Nonlinear Optics, The Sergei Akhmanov Memorial Volume* (CRC Press, 2021) pp. 17–25.

[5] V. Kozlov and J. Eberly, Opt. Commun. **179**, 85 (2000).

[6] D. M. Nguyen, C. Soci, and C. H. Ooi, Sci. Rep. **6** (2016), 10.1038/srep21083.

[7] D. Türkpençe and O. E. Müstecaplıoğlu, Phys. Rev. E **93**, 012145 (2016).

[8] F. Ciccarello, S. Lorenzo, V. Giovannetti, and G. M. Palma, Phys. Rep. **954**, 1 (2022).

[9] Z.-X. Man, Y.-J. Xia, and R. Lo Franco, Phys. Rev. A **97**, 062104 (2018).

[10] H. Pichler, T. Ramos, A. J. Daley, and P. Zoller, Phys. Rev. A **91**, 042116 (2015).

[11] V. Giovannetti and G. M. Palma, Phys. Rev. Lett. **108**, 040401 (2012).

[12] T. Ramos, H. Pichler, A. J. Daley, and P. Zoller, Phys. Rev. Lett. **113**, 237203 (2014).

[13] S. Cusumano, A. Mari, and V. Giovannetti, Phys. Rev. A **97**, 053811 (2018).

[14] S. Lorenzo, R. McCloskey, F. Ciccarello, M. Paternostro, and G. M. Palma, Phys. Rev. Lett. **115**, 120403 (2015).

[15] S. Lorenzo, A. Farace, F. Ciccarello, G. M. Palma, and V. Giovannetti, Phys. Rev. A **91**, 022121 (2015).

[16] C. Pellitteri, G. Palma, and S. Lorenzo, Phys. Scr. (2023).

[17] B.-G. Englert and G. Morigi, in *Coherent Evolution in Noisy Environments* (Springer Berlin Heidelberg, 2002) pp. 55–106.

[18] H.-P. Breuer, F. Petruccione, *et al.*, *The theory of open quantum systems* (Oxford University Press on Demand, 2002).

[19] P. Filipowicz, J. Javanainen, and P. Meystre, Phys. Rev. A **34**, 3077 (1986).

[20] P. Filipowicz, J. Javanainen, and P. Meystre, J. Opt. Soc. Am. B **3**, 906 (1986).

[21] Á. Rivas, S. F. Huelga, and M. B. Plenio, Rep. Prog. Phys. **77**, 094001 (2014).

[22] S. Richter and R. F. Werner, J. Stat. Phys. **82**, 963 (1996).

[23] D. Burgarth and V. Giovannetti, New J. Phys. **9**, 150 (2007).

[24] D. Burgarth, G. Chiribella, V. Giovannetti, P. Perinotti, and K. Yuasa, New J. Phys. **15**, 073045 (2013).

[25] M. O. Scully and M. S. Zubairy, *Quantum Optics* (Cambridge University Press, 1997).

[26] M. O. Scully, in *AIP Conference Proceedings*, Vol. 643 (American Institute of Physics, 2002) pp. 83–91.

[27] C. Gogolin and J. Eisert, Rep. Prog. Phys. **79**, 056001 (2016).

[28] C. L. Latune, I. Sinayskiy, and F. Petruccione, Quantum Sci. Technol. **4**, 025005 (2019).

[29] Z.-X. Man, Y.-J. Xia, and N. B. An, J. Phys. B: At. Mol. Opt. Phys. **53**, 205505 (2020).

[30] V. Giovannetti and G. M. Palma, J. Phys. B: At. Mol. Opt. Phys. **45**, 154003 (2012).

[31] M. Amniat-Talab, M. Saadati-Niari, S. Guérin, and R. Nader-Ali, Phys. Rev. A **83**, 013817 (2011), publisher: American Physical Society.

[32] G. Bevilacqua, G. Schaller, T. Brandes, and F. Renzoni, Phys. Rev. A **88**, 013404 (2013), publisher: American Physical Society.

[33] N. V. Vitanov, K.-A. Suominen, and B. W. Shore, "Creation of coherent atomic superpositions by fractional STIRAP," (1998), arXiv:quant-ph/9811079.

[34] N. Shirkhanghah, M. Saadati-Niari, and S. Ahadpour, Quantum Inf. Process. **19**, 128 (2020).

[35] M. Saadati-Niari and M. Amniat-Talab, J. Mod. Opt. **61**, 1492 (2014), publisher: Taylor & Francis _eprint: https://doi.org/10.1080/09500340.2014.942404.

[36] P. A. Ivanov, B. T. Torosov, and N. V. Vitanov, Phys. Rev. A **75**, 012323 (2007).

[37] W. H. Zurek, "Information transfer in quantum measurements: Irreversibility and amplification," in *Quantum Optics, Experimental Gravity, and Measurement Theory*, edited by P. Meystre and M. O. Scully (Springer US, Boston, MA, 1983) pp. 87–116.

[38] L. Henderson and V. Vedral, J. Phys. A: Math. Gen. **34**, 6899 (2001).

[39] W. H. Zurek, "Einselection and decoherence from an information theory perspective," in *Quantum Communication, Computing, and Measurement 3*, edited by P. Tombesi and O. Hirota (Springer US, Boston, MA, 2002) pp. 115–125.

[40] H. Ollivier and W. H. Zurek, Phys. Rev. Lett. **88**, 017901 (2001).

[41] L. Henderson and V. Vedral, J. Phys. A: Math. Gen. **34**, 6899 (2001).

[42] S. Luo, Phys. Rev. A **77**, 042303 (2008).

[43] A. Peres, Phys. Rev. Lett. **77**, 1413 (1996).

[44] M. Horodecki, P. Horodecki, and R. Horodecki, Phys. Lett. A **223**, 1 (1996).

[45] M. B. Plenio, Phys. Rev. Lett. **95**, 090503 (2005).